

Room Temperature Solid Surface Water with Tetrahedral Jumps of ^2H Nuclei Detected in $^2\text{H}_2\text{O}$ -Hydrated Porous Silicates

Alan J. Benesi,*[§] Michael W. Grutzeck,[#] Bernie O'Hare,[§] and John W. Phair[‡]

Department of Chemistry, The Pennsylvania State University, University Park, Pennsylvania 16802, Materials Research Laboratory, The Pennsylvania State University, University Park, Pennsylvania 16802, and Office of Infrastructure Research and Development, Federal Highway Administration, McLean, Virginia 22101

Received: May 6, 2004; In Final Form: July 15, 2004

The nature of water adjacent to solid silicate surfaces in kanemite, rehydrated zeolite A, rehydrated highly porous glass, rehydrated high surface area silica gel, and the hydration products of tricalcium silicate has been investigated with ^2H NMR techniques and calorimetry. The room temperature ^2H NMR quadrupole echo spectra of all samples show a sharp central resonance that corresponds to $^2\text{H}_2\text{O}$. The kanemite, porous glass, and silica gel spectra show in addition powder patterns that were assigned, based on previous findings for kanemite, to silanol $-\text{OH}$ groups experiencing rapid 3-fold jumps or rotational diffusion about the $\text{Si}-\text{O}$ bond. The spectrum of hydrated tricalcium silicate shows in addition to the aqueous peak a rigid powder pattern that is assigned to $\text{Ca}(\text{O}^2\text{H})_2$. Spectra obtained at -120 and -150 $^\circ\text{C}$ for the kanemite sample show that the qcc values for the aqueous deuterons range from 180 to 210 kHz, as would be expected for the different water environments observed in the X-ray structure of kanemite. Room temperature ^2H T_1 data obtained at two magnetic fields for kanemite are exactly matched with theoretical calculations that assume rapid tetrahedral jumps of the ^2H nuclei ($2.0 \times 10^8 \text{ s}^{-1}$) in a solid-state lattice similar to those observed in $^2\text{H}_2\text{O}$ ice below the freezing point. The T_1 data cannot be matched with isotropic rotational diffusion as would be expected for liquid water. The T_1 data for low loadings of $^2\text{H}_2\text{O}$ in zeolite A are also matched with the tetrahedral jump model. T_1 data for the other samples are consistent with rapid exchange of ^2H nuclei or $^2\text{H}_2\text{O}$ molecules between solid-state surface water experiencing rapid tetrahedral jumps and liquid-state water farther from the surface. Heat evolution observed during hydration of all samples is consistent with the heat of fusion expected for a liquid to solid phase transition for the surface water.

Introduction

Water occurring adjacent to solid surfaces has long been recognized for its anomalous behavior when compared to bulk water. Surface water has very short ^1H and ^2H NMR relaxation times, so a mechanism such as fast exchange of the surface water with bulk water further from the surface must be invoked to explain the relaxation times observed in hydrated solids.^{1–4} The nature of surface water has, however, remained clouded in controversy. The goal of the work reported here is to further elucidate the nature of surface water present in five hydrous silicates with use of deuterium NMR.

Deuterium (^2H) NMR is particularly advantageous for characterizing molecular motions in liquids or solids.^{5,6} The ^2H quadrupolar interaction is so large that other interactions, such as the ^2H chemical shift and $^2\text{H}-^2\text{H}$ homonuclear dipolar interactions, can usually be neglected. Paramagnetic interactions can have a significant effect, but can be avoided if pure substances without paramagnetic impurities are used. In the absence of molecular motion other than vibrations and librations, the “rigid” solid state ^2H powder spectrum is characterized by the quadrupole coupling constant ($\text{qcc} = e^2qQ/h$), typically between 160 and 300 kHz, and an asymmetry parameter η , typically close to zero due to the axial symmetry of the single

covalent bond to an H atom. The quadrupolar interaction provides a direct link between the observed ^2H spectral frequency and the orientation of the covalent bond relative to the ^2H nucleus. In powder samples (including the hydrated silicate samples studied here) there is a statistical ensemble of randomly oriented small crystals and particles with corresponding randomly oriented covalent bonds and a corresponding range of ^2H frequencies that yield a characteristic ^2H “powder spectrum” with a width of 1.5 times the value of the qcc.

If molecular and atomic motion causes the ^2H covalent bonds to reorient much more slowly than the qcc, the sample is said to be “rigid” on the ^2H NMR time scale, and the powder spectrum is not directly affected. In the context of ^2H NMR, “rigid” means that the positions of the water molecules and their deuterium nuclei are fixed in the crystal lattice except for small-amplitude vibrations, torsional oscillations, and occasional ($\nu < 10^4 \text{ s}^{-1}$) large-amplitude jumps.^{7,8} Even for “rigid” samples the geometry and rate of motion can be investigated with ^2H NMR by application of the spin alignment pulse sequence and its two-dimensional versions.^{9,10} Faster motions comparable to or faster than the qcc directly affect the ^2H NMR powder spectrum and ^2H NMR T_1 and T_2 relaxation times.^{11,12} Because of this sensitivity to motion, ^2H NMR can be used to characterize motions with frequencies ranging from $\sim 1 \text{ s}^{-1} < \nu < 10^{13} \text{ s}^{-1}$.

Dynamics of Water in Crystalline Solids. For some crystalline hydrates such as $\text{K}_2\text{C}_2\text{O}_4 \cdot 2\text{H}_2\text{O}$, $\text{LiO}^2\text{H} \cdot 2\text{H}_2\text{O}$, and $\text{Sr}(\text{HCOO})_2 \cdot 2\text{H}_2\text{O}$, rigid powder ^2H NMR spectra are observed at room temperature. In other crystalline hydrates such as Li_2 -

* To whom correspondence should be addressed. E-mail: alan@chem.psu.edu.

[§] Department of Chemistry, The Pennsylvania State University.

[#] Materials Research Laboratory, The Pennsylvania State University.

[‡] Federal Highway Administration.

TABLE 1: Sources of Starting Materials and Amounts Used for Kanemite Synthesis

compd and source	weight, g			equivalent moles		
	δ -Na ₂ Si ₂ O ₅ Clariant SKS-6	silica gel Merck 70–230	² H ₂ O Aldrich 99.9%	δ -Na ₂ Si ₂ O ₅ Clariant SKS-6	silica gel Merck	² H ₂ O Aldrich 99.9%
NMR experiments	1.81	1.19	1.59 ² H ₂ O	0.00994	0.0198	0.0794
calorimetry experiments	0.226	0.149	0.188 ¹ H ₂ O DI	0.00124	0.00248	0.01044

SO₄·2H₂O, Ba(ClO₃)₂·2H₂O, and CaSO₄·2H₂O, characteristic powder line shapes in ²H NMR spectra at room temperature show that the two ²H nuclei in a given hydrate water molecule interchange positions rapidly ($\nu > 10^6$ s⁻¹).^{7,8} This is achieved either by rapid 180° jump motions of the intact water molecule about the C₂ symmetry axis, or by jumps of the ²H nuclei between the two equivalent covalent bonds to oxygen.^{7,8} However, if the latter hydrates are cooled to sufficiently low temperatures, the jump rate slows sufficiently to yield a rigid powder line shape.^{7,8} The two types of behavior therefore actually represent a continuum in which the measured C₂ symmetry jump rate is a direct reflection of the lattice energy of the hydrate and consequently the mobility of the ²H nuclei at a given temperature.

In contrast, water in the solid state (i.e. ice) has distinctly different dynamics. In ice that forms at the freezing point at atmospheric pressure (ice I_h), both ¹H and ²H NMR techniques show that *hydrogen nuclei experience tetrahedral jumps* around the oxygen atoms in the crystal lattice.^{10,13} The jumps are thought to be caused by diffusion of Bjerrum defects in the ice lattice.¹³ The jump rate is sufficiently fast even at 10 °C below the freezing point that the solid state ¹H or ²H NMR spectrum shows a single isotropic peak visually indistinguishable from that of liquid ^{1,2}H₂O.¹³

Description of Materials Studied. Five ²H₂O-containing silicates have been included in the study: two are layer structured silicates produced by the hydration of reactive solids with deuterated water, while the remaining three are well-known desiccants that were dried and then allowed to adsorb deuterated water.

Kanemite (NaHSi₂O₅·3H₂O) consists of alternating single layer sheets of [Si₂O₄OH]_nⁿ⁻, hydrated sodium ions, and interlayer water molecules.^{14–16} The silicon in the silicate layers is known from solid state ²⁹Si NMR to be exclusively Q³, meaning that each silicon atom is bonded to three other silicon atoms in the silicate sheet via oxygen atoms.^{14–16} The fourth bond for each silicon is to –OH or –O⁻.¹⁵ Na⁺ ions in kanemite form hydrates with the water between silicate layers, and may coordinate to the silicate lattice as well as to the water.^{14–16} The hydrated Na⁺ ions are fixed in the crystal lattice as shown by both X-ray diffraction and solid state ²³Na NMR.^{14–16} The X-ray structure shows that some of the oxygen atoms of the water molecules in kanemite are fixed, and some of the H–O–H bond angles and O–H bond lengths are unusually small.¹⁵ High atomic-displacement parameters for the H atoms indicate a heterogeneous distribution of water vacancies in hydration of Na⁺.¹⁵ The space between adjacent silicate layers in kanemite is 10.3 Å,^{15,16} so no water molecules are located farther than about 5.2 Å from a silicate surface.

Calcium silicate hydrate (nominally 1.7CaO·SiO₂·2–4H₂O) forms during setting and hardening of hydrated Ca₃SiO₅.¹⁷ Although it is X-ray amorphous, there is anecdotal evidence that suggests that calcium silicate hydrate has a layer structure similar to 1.1 nm tobermorite (Ca₅Si₆O₂₂·10H₂O) and as such contains highly disorganized silicate sheets separated by interlayers containing calcium ions, OH⁻, and water molecules.¹⁸

Calcium silicate hydrate typically has surface areas in the range of 100 m²/g.

The three desiccants studied were the following: zeolite A (Na₁₂[Al₁₂Si₁₂O₄₈]·27H₂O) a well-known framework zeolite, Thirsty Glass (~99 wt % SiO₂), a highly porous leached precursor of Vycor glass, and a commercially available high surface area silica gel (SiO₂·xH₂O).

In the room temperature hydrated silicate samples investigated here, molecular motions at room temperature have $\nu \gg$ qcc as determined from ²H spectra and ²H NMR T₁ relaxation times. A new model for the nature of the water at the surface is derived that suggests that at least part of the water is solid, with the ²H nuclei experiencing rapid tetrahedral jumps similar to those observed in ice below the freezing point.

Experimental Methods

Five dry starting materials were mixed with deuterated water and allowed to either hydrate with or adsorb the water and form the hydrous materials studied here with ²H NMR techniques. In each case a significant amount of heat is given off during the reaction. Calorimetric measurements were also obtained for each set of reactants to validate or refute the hypothesis that surface water may be in the solid state. Some of the heat evolved during hydration may be heat of fusion for the liquid to solid change in state of the surface water. In addition, some of the samples were characterized by using X-ray diffraction. Details are given below.

Sample Preparation. Kanemite was synthesized by adding either ²H₂O (NMR) or ¹H₂O (calorimetry) to a mixture of δ -Na₂Si₂O₅ and silica gel, mixing it and allowing it to hydrate at 21 °C as a function of time. See Table 1 for sources of materials and amounts used. In both cases, the powdered starting materials were first dry-mixed to ensure that components were homogeneous before combining them with water at a mole ratio of δ -Na₂Si₂O₅:SiO₂:water of 1:2:8. Although the stoichiometric composition for kanemite is Na₂O·4SiO₂·7H₂O, a slight excess of water was added to enable more uniform mixing and to allow for inevitable evaporation during sample preparation. After preparation, samples were stored in sealed vials at 21 ± 1 °C in the tightly controlled environment of the NMR facility. For the sake of comparison, the sample formulation studied here is identical with samples undergoing concurrent quasielastic neutron scattering experiments.¹⁹

Calcium silicate hydrate (C–S–H) is a gellike layer structured hydrate that forms in direct response to the hydration of Ca₃SiO₅. The tricalcium silicate was synthesized in house from reagent grade CaCO₃ (Aldrich) and silica (various sources) mixed in a molar ratio of 3:1 and fired at increasingly higher temperatures with a final firing at 1600 °C. The X-ray diffraction powder pattern was used to verify the structure. The tricalcium silicate is predominantly triclinic but contains a trace of monoclinic Ca₃SiO₅. Finely powdered samples (50–100 μm) were mixed with ²H₂O (NMR) and ¹H₂O (calorimeter) and allowed to hydrate at room temperature as a function of time. The experimental details for the ²H₂O hydration studies of Ca₃SiO₅ have been described previously.¹⁷ For this study, however,

a single sample with an $^2\text{H}_2\text{O}/\text{Ca}_3\text{SiO}_5$ ratio of 0.50 by weight that was prepared six years ago and stored in a sealed vial at $21 \pm 1^\circ\text{C}$ was recovered and examined.

Phase pure zeolite A ($\text{Na}_{12}\text{Al}_{12}\text{Si}_{12}\text{O}_{48} \cdot 27\text{H}_2\text{O}$) was purchased from Aldrich Chemical Co. It was calcined at 500°C for 2 h to completely remove its hydration water, and stored in a desiccator until used in the calorimetry and NMR experiments. Three rehydrated samples were prepared for NMR experiments with $^2\text{H}_2\text{O}/\text{zeolite}$ ratios of 0.50, 0.050, and 0.005 by weight, respectively.

Highly porous glass ("Thirsty Glass", Code 7930) was purchased from Corning Glass. It is prepared by leaching a two-phase glass with water to remove the soluble phase leaving behind a porous glass having a network of 4-nm pores (28 vol %) embedded in a 99.9 wt % silica glass. The internal surface area of the glass is $250\text{ m}^2/\text{g}$. Thirsty Glass is sold by Corning as an adsorbent for all types of airborne contaminants (organics, gases, water vapor) to protect delicate electronic instruments. Thirsty Glass is also the unfired precursor for making Vycor Glass. In preparation for our experiments, the sample was purged of its adsorbed organic content by grinding it, soaking the powder in concentrated nitric acid containing a trace of sodium chlorate, and then washing the powder repeatedly with distilled water as per Corning's cleaning instructions. It was then dried at 500°C for an hour and stored in a desiccator until used. Two samples were prepared for NMR experiments with $^2\text{H}_2\text{O}/\text{glass}$ ratios of 0.5 and 0.005 by weight, respectively.

Silica gel (60–200 mesh, average particle diameter 63–200 μm , mean pore diameter 150 Å) was purchased from J. T. Baker Chemical Co., dried at 335°C for 45 min, and stored in a desiccator until used. A single sample was hydrated for NMR study with use of an $^2\text{H}_2\text{O}/\text{silica}$ gel ratio of 0.0125 by weight.

NMR Techniques. ^2H NMR experiments were carried out at two magnetic fields, 6.98 T (45.65 MHz) and 11.75 T (76.78 MHz), on Chemagnetics CMX-300 and Bruker AMX-2–500 spectrometers, respectively, at the tightly controlled ambient temperature of the NMR facility, $21 \pm 1^\circ\text{C}$. The quadrupole echo pulse sequence was used to obtain ^2H spectra at 45.65 MHz for all samples ($\pi/2 = 1.9\text{ }\mu\text{s}$, $\tau_1 = 30\text{ }\mu\text{s}$, $\tau_2 = 25\text{ }\mu\text{s}$). The T_1 values of the central aqueous peaks were determined with the inversion recovery pulse sequence at both frequencies. In some cases the T_1 values were determined with the inversion recovery quadrupole echo pulse sequence. Low-temperature quadrupole echo spectra were obtained by using the variable-temperature apparatus of the Chemagnetics CMX-300. Temperature calibration with a thermocouple taped in place in the probe sample coil verified that the temperatures were accurate to $\pm 2^\circ\text{C}$ down to -150°C .

Theoretical ^2H NMR powder line shape simulations^{20,21} and relaxation times^{11,12} were calculated with Mathematica programs developed by the authors. These programs are available as a ZIP file in the Supporting Information. Because the motions either had frequencies much greater or much less than the qcc, the powder line shapes simulated in both cases were independent of the specific jump rate.²⁰ No corrections to the experimental or calculated spectra were made for finite pulse width effects, since these are expected to be negligible except for outermost shoulders (parallel edges) of the widest powder patterns.²² T_1 relaxation times for solid-state jump motions were calculated by using the formalism developed by Torchia and Szabo.¹¹ T_1 relaxation times for liquid-state isotropic rotational diffusion were calculated by using the equations derived by Sudmeier et al.¹²

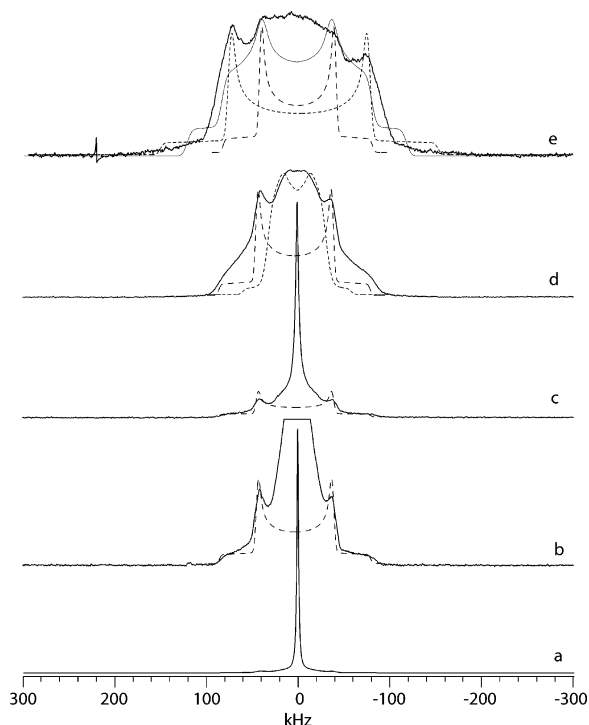


Figure 1. ^2H quadrupole echo spectra of kanemite prepared with $^2\text{H}_2\text{O}$: (a) at room temperature 10 days after mixing reactants; (b) vertical expansion of spectrum a, with a simulation (coarse dashed line) of silanol ($\text{Si}-\text{O}-^2\text{H}$) groups experiencing rapid rotational diffusion or rapid 120° jumps about the $\text{Si}-\text{O}$ bond axis for an $\text{Si}-\text{O}-\text{H}$ bond angle of 143° , $q_{\text{cc}} = 240\text{ kHz}$, $\eta = 0$; (c) at room temperature after evaporative loss from heating in air at 40°C for 3 h, with a simulation (coarse dashed line) of silanol motion as in spectrum b; (d) at room temperature after evaporative loss from heating in air at 80°C for 3 h, with a simulation (coarse dashed line) of silanol motion as in spectrum b, and a simulation (fine dashed line) showing the spectrum calculated for rapid jumps of distorted tetrahedral symmetry between four sites with polar angles $\theta = 0^\circ$, $\phi = 0^\circ$; $\theta = 81^\circ$, $\phi = 0^\circ$; $\theta = 90^\circ$, $\phi = 120^\circ$; $\theta = 109.47^\circ$, $\phi = 240^\circ$, $q_{\text{cc}} = 193\text{ kHz}$, $\eta = 0.8$ (this simulation is merely an example of many possible distorted tetrahedral jump powder patterns that could be used to fit the central feature in the spectrum); (e) at -120°C , with a simulation (fine dashed line) for rigid ^2H with $q_{\text{cc}} = 205\text{ kHz}$ and $\eta = 0$, another simulation (coarse dashed line) of silanol motion as in spectrum b, and a third simulation (fine solid line) of rapid C_2 symmetry jumps, HOH bond angle = 130° , $q_{\text{cc}} = 220\text{ kHz}$, $\eta = 0$; a fourth simulation (not shown) of rapid C_2 symmetry jumps with HOH bond angle = 90° is almost identical with that for the silanol motion (coarse dashed line) and also matches the outer part of the central feature.

Calorimetry. Calorimetric data for most of the samples were obtained on a Thermochemical Seebeck envelope isothermal calorimeter at 25°C . The data for kanemite were obtained on a TA Instruments 2920 Modulated DSC, using Thermal Solutions software to monitor isothermal heat evolution at 25°C .

Results and Discussion

Kanemite Spectral Analysis. The room temperature ($21 \pm 1^\circ\text{C}$) ^2H quadrupole echo spectrum obtained at 45.65 MHz for kanemite prepared with $^2\text{H}_2\text{O}$ is shown in Figure 1a,b. A large, relatively sharp isotropic peak as well as a much weaker, axially symmetric ^2H powder pattern is present in the spectrum. The sharp peak is assigned to the $^2\text{H}_2\text{O}$ interlayer aqueous solution. The peak width at half-height for this resonance at both magnetic fields is shown in Table 2. The ^2H chemical shift of the aqueous peak is known from ^1H NMR to be 5 ppm.¹⁴ It is apparent from Figure 1b that the weak axially symmetric powder pattern is shifted downfield with respect to the water peak as was observed

TABLE 2: T_1 Data and Calorimetry Data

sample ^a	² H ₂ O to solid ratio, by wt	$\Delta H_{\text{hydration rxn}}$, cal/g of ¹ H ₂ O ^a	$\Delta\nu_{1/2}$, kHz (45.65 MHz)	$\Delta\nu_{1/2}$, kHz (76.78 MHz)	T_1 , ms (45.65 MHz) ^a	T_1 , ms (76.78 MHz) ^a	χ_{solid} in the aq phase ^b
kanemite	0.53	−1136	1.6	1.8	4.2	6.2	1
kanemite ^c	0.50	N/A	3.3	3.2	4.6	6.8 ^d	1
kanemite ^e	0.37	N/A	narrow powder pattern	N/A	7 (central powder pattern)	N/A	1
zeolite a/ ^f	0.50	−110	0.4	N/A	17.3	N/A	0.24
	0.05	N/A	1.7	1.4	8.3	9.2	0.58 ^g
	0.005	N/A	4.1	N/A	5.9	N/A	0.71 ^g
Thirsty Glass ^h	0.50	−1.5	1.2	N/A	138	N/A	0.02
	0.005	N/A	0.9	0.8	17.4	18.5	0.27
Ca ₃ SiO ₅	0.50 (6 days after mixing)	−96 ⁱ	1.0	N/A	33	N/A	0.12
	0.50 (1 month after mixing)	N/A	3.2	N/A	13	N/A	0.32
	0.50 (6 years after mixing)	N/A	3.9	1.6	12.8	26	0.27
silica gel (Baker)	0.0125	−43	0.6	0.3	27.8	27.2	0.17

^a All samples were stored in sealed containers at 21 ± 1 °C. All NMR measurements were carried out at 21 ± 1 °C unless otherwise noted. T_1 values reported are those for the central sharp aqueous peak. All isothermal calorimetry experiments were carried out at 25 °C. ^b Mole fractions of the ice-like aqueous phase were calculated from eq 1 assuming that the T_1 values were the same as those observed for kanemite at the same magnetic field. When data at both magnetic fields were available, the average of the two results is reported. ^c After evaporative loss of ²H₂O in air at 40 °C for 3 h. ^d T_1 determined at 25 °C. ^e After evaporative loss of ²H₂O in air at 80 °C for 3 h. ^f Calcined in air at 500 °C for 2 h before hydration. ^g It is likely that the mole fraction of ice-like water is actually 1 for these samples (see text). ^h Washed with concentrated HNO₃ containing dilute sodium chlorate, then rinsed extensively with distilled water, then calcined at 500 °C for 1 h before hydration. ⁱ In this case the heat evolved during setting, between 3 and 7 days after mixing. In this case, ²H₂O was used for the calorimetry experiments.

with ¹H NMR for silanol −OH in kanemite.¹⁴ The limited width of the weaker powder pattern (77 kHz between the perpendicular edges, indicating an apparent qcc = 103 kHz and $\eta \approx 0$) indicates molecular motion for the corresponding ²H. The apparent qcc of 103 kHz and near axial symmetry is consistent with either rapid three site jumps or rapid rotational diffusion of the O−²H bond (both models give the same result) about the Si−O torsion angle with an Si−O−²H bond angle of 143°, assuming that the rigid qcc is 240 kHz^{20,21} (Figure 1b, coarse dashed line). The low intensity powder pattern is therefore assigned to ²H experiencing three site jumps or rotational diffusion of the OH bond about the Si−O bond in silanol groups. Since a distinct powder pattern is obtained for the silanol −OH, ²H exchange between the silanol −OH and the interlayer aqueous solution is slow ($\nu_{\text{exchange}} < \text{qcc}$).

For the sharp aqueous peak, unequivocal determination of the water dynamics is not possible by simple inspection. Either isotropic liquid-state rotational diffusion or rapid high-symmetry (tetrahedral or octahedral) jump motions can produce a single isotropic line. Rapid tetrahedral jumps produce a single sharp line if $\eta = 0$ and a sharp peak that is actually a “mini-powder pattern” if η is nonzero.^{13,17} Less symmetric types of rotational diffusion and jump motions cannot account for the observed spectrum because these would produce characteristic powder patterns in the ²H spectrum, not a single sharp peak.^{20,21}

Figure 1e shows the ²H quadrupole echo spectrum at 45.65 MHz obtained for kanemite at −120 °C. The sharp central aqueous peak has been replaced by a superposition of different ²H NMR powder patterns as would be expected for the different environments of hydrogen in crystalline kanemite.^{14–16} Spectra obtained at −150 °C (not shown) are virtually identical. The outer (parallel) edges of the powder spectrum have been attenuated by finite pulse width effects,²² but no corrections were made since the lack of intensity does not affect the spectral analysis. The outer horn maxima (perpendicular edges) at 73.8 and −71.0 kHz are consistent with qcc = 193 kHz and $\eta \approx 0$, although the breadth of the horns is consistent with a range of qcc values between 175 and 210 kHz and η values less than

0.2. This falls in the expected range for rigid hydrates.^{7,8} A simulation with qcc = 205 kHz, $\eta = 0$, and 4 kHz of Gaussian broadening (Figure 1e, fine dashed line) provides a good match for the outer horns, although both lower and higher qcc values are evident from the higher intensity both inside and outside the simulated horns. The variability in the qcc values may be a manifestation of the variability of H−O−H bond angles and O−H bond lengths observed in kanemite.¹⁵ The central feature between the outer horns may contain contributions from rapid low-temperature three-site jumps or rotational diffusion of the OH bond in silanol groups about the Si−O bond (Figure 1e, coarse dashed line) but with wider variability of the Si−O−H bond angles than observed at room temperature. It may also contain contributions from rapid C_2 symmetry jumps of H in the hydrate water molecules^{7,8} of Na(H₂O)_n⁺ ($n \leq 6$, Figure 1e, thin solid line) but with wider variability of the H−O−H bonds as would be expected for kanemite.¹⁵

The ²H quadrupole echo spectra at 45.65 MHz shown in spectra c and d in Figure 1 represent changes in kanemite brought about after two previously sealed hydrated kanemite samples were opened and heated in air for 3 h at 40 and 80 °C, respectively, cooled, resealed, and stored at 21 °C in a desiccator prior to reexamination. These spectra show loss of intensity from both the sharp aqueous peak and the powder pattern for dynamic silanol due to evaporative loss of water (Figure 1c, coarse dashed line). The central aqueous powder pattern remaining after heating to 80 °C is assigned to strongly bound hydrate water in which the ²H nuclei experience rapid jumps of distorted but nearly tetrahedral symmetry (Figure 1d, fine dashed line).

Calcium Silicate Hydrate Spectral Analysis. NMR assignments for hydrated Ca₃SiO₅ have been reported previously.¹⁷ The quadrupole echo ²H spectrum of a set and hardened hydrated Ca₃SiO₅ sample shows in addition to the aqueous peak a broad axially symmetric powder pattern with horns at ± 98 kHz that is assigned to rigid Ca(O²H)₂¹⁷ (Figure 2d). The powder pattern was well matched with a simulation using qcc = 262 kHz, $\eta = 0$ (Figure 2d, coarse dashed line). No correction was made to either the experimental or calculated powder spectrum

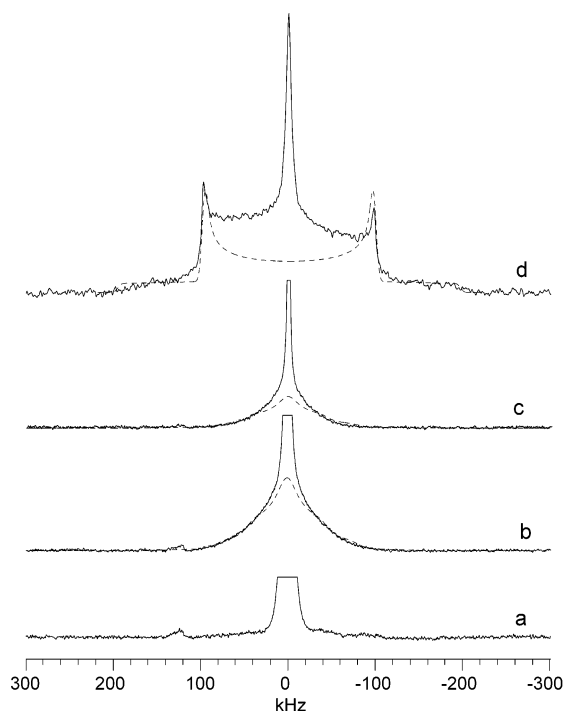


Figure 2. ^2H quadrupole echo spectra of: (a) zeolite A hydrated with $^2\text{H}_2\text{O}$, 0.005 g of $^2\text{H}_2\text{O}$ per 1 g of zeolite A; (b) highly porous Corning "Thirsty" Glass hydrated with $^2\text{H}_2\text{O}$, 0.005 g of $^2\text{H}_2\text{O}$ per 1 g of porous glass, with a simulation (coarse dashed line) of silanol ($\text{Si}-\text{O}-^2\text{H}$) groups experiencing rapid rotational diffusion or rapid 120° jumps about the $\text{Si}-\text{O}$ bond axis for a sum of an equally weighted set of spectra with a range of $\text{Si}-\text{O}-\text{H}$ bond angles from 90° to 165° ($qcc = 240$ kHz, $\eta = 0$); (c) silica gel hydrated with $^2\text{H}_2\text{O}$, 0.0125 g of $^2\text{H}_2\text{O}$ per 1 g of silica gel, with a simulation (coarse dashed line) of silanol motion as in spectrum b; (d) Ca_3SiO_5 hydrated with $^2\text{H}_2\text{O}$, 0.50 g of $^2\text{H}_2\text{O}$ per 1 g of Ca_3SiO_5 , 3 months after mixing, fully set and hardened (the coarse dashed line shows a simulation of the powder pattern with $qcc = 262$ kHz, $\eta = 0$, corresponding to rigid $\text{Ca}(\text{O}^2\text{H})_2$).

for finite pulse width effects²² since the loss of intensity from the outer (parallel) edges does not affect the results.

Zeolite A Spectral Analysis. Only the sharp aqueous peak appears in the ^2H quadrupole echo spectrum of zeolite A at all loadings. The lack of a powder line shape in the lowest loading zeolite A spectrum (Figure 2a) is consistent with its known lack of silanol groups.

Thirsty Glass Spectral Analysis. A sharp aqueous peak dominates the ^2H quadrupole echo spectra obtained at 21°C for porous glass at both loadings of $^2\text{H}_2\text{O}$. Careful inspection of the expansion obtained for the lowest loading reveals in addition to the dominant aqueous peak a broad triangular peak (Figure 2b) that is assigned to silanol $-\text{OH}$ experiencing rapid rotational diffusion or 3-fold jumps around the $\text{Si}-\text{O}$ bond. By assuming a range of allowable $\text{Si}-\text{O}-\text{H}$ bond angles between 90° and 165° and a rigid qcc of 240 kHz it is possible to simulate this broad triangular peak (Figure 2b, coarse dashed line). Quadrupole echo spectra obtained at 30, 40, and 50°C show no changes in the broad triangular peak relative to the aqueous peak. This suggests that the triangular peak does not arise from molecular motions with frequencies comparable to qcc ($\nu \approx qcc$), since such intermediate rate motions would be expected to produce powder spectra that depend strongly on temperature. In accordance with the observations for kanemite, the aqueous deuterium nuclei do not exchange rapidly with the silanol $-\text{OH}$ groups.

Silica Gel Spectral Analysis. The ^2H quadrupole echo spectrum obtained at 21°C for rehydrated silica gel shows in

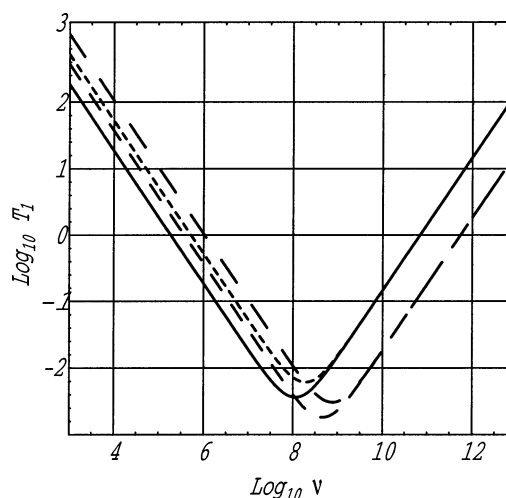


Figure 3. Plot of the theoretical dependence of ^2H T_1 on the tetrahedral jump rate,¹¹ ν (s^{-1}), and on the inverse of the rotational correlation time¹² $1/\tau_c$ assuming $qcc = 193$ kHz, $\eta = 0$. $\text{Log}(T_1)$ is plotted against $\text{log}(\nu)$ or $\text{log}(1/\tau_c)$. The solid and fine dashed lines respectively show the values calculated for tetrahedral jumps at 45.65 and 76.78 MHz (6.98 and 11.75 T). The medium coarse and very coarse dashed lines respectively show the values calculated for isotropic rotational diffusion at 45.65 and 76.78 MHz.

addition to the dominant aqueous peak a broad triangular peak (Figure 2c) that is assigned to silanol $-\text{OH}$ experiencing rapid rotational diffusion or 3-fold jumps about the $\text{Si}-\text{O}$ bond. As in the case of porous glass, a range of $\text{Si}-\text{O}-\text{H}$ bond angles from 90° to 165° and a qcc of 240 kHz is assumed in the simulation. No changes in the broad triangular peak relative to the aqueous peak were observed at 50°C . Again, the aqueous deuterium nuclei do not exchange rapidly with the silanol $-\text{OH}$ groups.

Kanemite T_1 and Calorimetry Analysis. ^2H NMR T_1 relaxation measurements for the central sharp aqueous peak were used to elucidate the nature of molecular motion of aqueous deuterons in room temperature kanemite.^{11,12} The relaxation data are reported in Table 2. The theoretical T_1 dependence of kanemite was calculated by using two different models: isotropic liquid-state rotational diffusion¹² and solid-state tetrahedral jumps¹¹ assuming an average $qcc = 193$ kHz and $\eta = 0$ based on the observations for kanemite at low temperature. The results are shown in Figures 3 and 4. For comparison, bulk $^2\text{H}_2\text{O}$ at 21°C has $qcc = 216$ kHz and $\eta = 0.1$,¹³ and an experimental inversion recovery T_1 value of 0.41 ± 0.01 s at 45.65 MHz and 0.38 ± 0.01 s at 76.78 MHz. The experimental T_1 values for bulk $^2\text{H}_2\text{O}$ correspond closely to values calculated with the isotropic rotational diffusion model if $\tau_c = 3.5 \pm 0.3 \times 10^{-12}$ s (or $1/\tau_c = 2.9 \times 10^{11}$ Hz).

For kanemite, the experimental ^2H T_1 values for the sharp aqueous peak (Table 2) at 21°C and 45.65 MHz fell rapidly from those of bulk $^2\text{H}_2\text{O}$ to 13 ms 2 h after preparation and 6 ms 16 h after preparation, and then stabilized after several days at 4.2 ± 0.5 ms at 45.65 MHz and 6.2 ± 0.5 ms at 76.78 MHz. Only the stabilized T_1 values for kanemite are shown in Table 2. All inversion recovery T_1 data sets for kanemite were well matched with a single exponential.

Comparison of the experimental T_1 values with the calculated values in Figures 3 and 4 shows that the magnetic field dependence of the T_1 values is consistent only with the solid-state tetrahedral jump model. For $qcc = 193$ kHz and $\eta = 0$ the liquid-state isotropic diffusion model predicts either too small of a change in T_1 with Larmor frequency (from 4.2 to 4.6 ms)

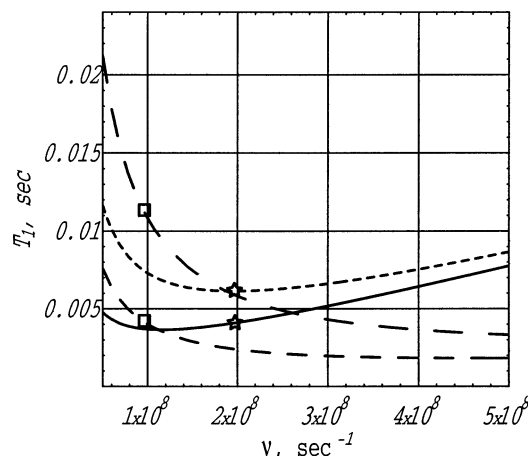


Figure 4. Expanded view of a plot of the theoretical dependence of ^2H T_1 on the tetrahedral jump rate,⁹ ν (s^{-1}), and on the isotropic rotational diffusion coefficient¹⁰ $1/\tau_c$ assuming $q_{cc} = 193$ kHz, $\eta = 0$. T_1 is plotted against ν or $1/\tau_c$. The solid and fine dashed lines respectively show the dependence calculated for tetrahedral jumps at 45.65 and 76.78 MHz (6.98 and 11.75 T). The medium coarse and very coarse dashed lines respectively show the dependence calculated for isotropic rotational diffusion at 45.65 and 76.78 MHz. Stars indicate where the calculated and experimental values for the tetrahedral jump model match exactly. Squares show that the isotropic rotational diffusion model cannot match both experimental values simultaneously.

at about $1/\tau_c = 2.2 \times 10^9$ Hz or too large a change (from 4.2 to 11.4 ms with $1/\tau_c = 9.5 \times 10^7$ Hz, Figure 4). In contrast, with the same q_{cc} and η value the solid-state tetrahedral jump model exactly matches the experimental T_1 values at both magnetic fields for a jump rate of 2.0×10^8 Hz (Figure 4). The q_{cc} and η value used in the simulations are consistent with the range of q_{cc} values and small η value observed for the aqueous deuterons in the low-temperature powder spectrum of kanemite. Furthermore, the ability to use the tetrahedral jump model to simulate the T_1 values within experimental error covers a range of q_{cc} values from about 205 to 180 for $\eta = 0.1$ or less. An average effective q_{cc} and η are expected for an ensemble of aqueous ^2H nuclei jumping rapidly from tetrahedral site to tetrahedral site in solid water coordinated to Na^+ and hydrogen bonded to the silicate surface. The agreement between theory and experiment provides compelling evidence for solid water with rapid tetrahedral jumps of the H nuclei between the silicate layers in kanemite.

Approximate T_1 values were also determined for the silanol powder pattern (Figure 1b) of kanemite at 21 ± 1 °C. The T_1 values for the horns of the pattern were 175 ± 25 ms, again showing that there is not fast exchange between the powder pattern and the sharp central aqueous peak.

Recent quasielastic neutron scattering (QENS) experiments on an identical kanemite preparation prepared with $^1\text{H}_2\text{O}$ showed that the “bound water index” approached unity at the same time as the ^2H T_1 value approached its limiting value in the NMR experiments.¹⁹ The “bound water” detected by QENS is therefore assigned to the translationally hindered solid interlayer water and silanol $-\text{OH}$. It is interesting that “bound water” on the QENS time scale is dynamic on the ^2H NMR time scale with tetrahedral jumps or jumps around the Si–O bond angle at frequencies $\nu > q_{cc}$ at room temperature.

Isothermal calorimetry for the kanemite reaction showed that heat evolution lasted for several hundred minutes after addition of $^1\text{H}_2\text{O}$ to the dry reactants. The average of two runs yielded $\Delta H = -1585$ J/g (reactants) = -379 cal/g (reactants) or -1136 cal/g (H_2O). By comparison, $\Delta H_{\text{fusion}} = -79.72$ cal/g for $^1\text{H}_2\text{O}$

and -75.8 cal/g for $^2\text{H}_2\text{O}$.²³ Although the heat evolved during kanemite formation includes contributions from several processes such as adsorption, solvation of sodium ions, Si–O bond breaking (for SiO_2), and Si–O bond making (for $\delta\text{-Na}_2\text{Si}_2\text{O}_5$), more than enough heat is evolved to include a contribution from a change in state of water from liquid to solid.

Ca_3SiO_5 T_1 and Calorimetry Analysis. ^2H NMR T_1 relaxation times for the sharp central peak of the hydrated Ca_3SiO_5 spectrum are given in Table 2. It is noteworthy that the data no longer fit the tetrahedral jump model perfectly. A hypothesis consistent with the T_1 values is that the water in immediate contact with solid surfaces is solid with the ^2H nuclei experiencing rapid tetrahedral jumps, but that it is in rapid exchange with the remaining liquid water farther from the solid surfaces. In its simplest form, this model predicts

$$(1/T_n)_{\text{observed}} = \chi_{\text{solid}}(1/T_n)_{\text{solid}} + \chi_{\text{liquid}}(1/T_n)_{\text{liquid}} \quad (1)$$

where $n = 1$ or 2 for T_1 or T_2 relaxation, χ_{solid} = mole fraction of water that is solid experiencing rapid tetrahedral jumps of the H nuclei, $(1/T_n)_{\text{solid}}$ = inverse of the ice-like relaxation time, $T_{n,\text{solid}}$, $\chi_{\text{liquid}} = (1 - \chi_{\text{solid}})$ = mole fraction of liquid-state pore water, and $(1/T_n)_{\text{liquid}}$ = inverse of the liquid-state pore water relaxation time $T_{n,\text{liquid}}$. In samples where water cannot exchange rapidly between different pores or channels, eq 1 applies only to a particular pore or channel, and a sum over all pores and channels must be taken.

The fast exchange hypothesis has been used widely to explain experimental NMR relaxation times for hydrated solids, including clays, silica gel, porous glass, and cement.^{1–4} It has long been recognized that a fraction of the water in hydrated porous solids has a very short ^1H or ^2H NMR relaxation time, and that this water must be in fast exchange with the remaining liquid water to explain the observed relaxation times. The fast-relaxing water has been called surface water, bound water, immobile water, and even rigid water. Applicability of eq 1 requires that the surface water must itself be mobile on the ^2H NMR time scale, because water that is rigid on the NMR time scale ($\nu \ll q_{cc}$) cannot, by definition, participate in fast exchange. *The main difference between our model and earlier fast exchange models is that the water adjacent to solid silicate surfaces is identified specifically as solid state with the H nuclei experiencing rapid tetrahedral jumps.*

The presence of solid-state water in which the H nuclei experience rapid tetrahedral jumps is also supported by other observations for hydrated Ca_3SiO_5 . Heat evolution, changes in T_1 values, and the initial hardening of the mixture, called setting, occur about 4–6 h after mixing with $^1\text{H}_2\text{O}$ but take much longer after mixing with $^2\text{H}_2\text{O}$ at room temperature.^{17,24} This kinetic isotope effect is consistent with the essential role of $-\text{OH}$ bond breaking that is required for rapid tetrahedral jumps in the solid state.

The calorimetric data obtained for $^1\text{H}_2\text{O}$ hydrated Ca_3SiO_5 are shown in Table 2. In this case, the heat evolution observed is significantly greater than the heat of fusion of water.²³ Although there may be other contributions to the observed heat evolution, enough heat is released to contain contributions from the liquid- to solid-phase transformation of water during initial setting and hardening.

Zeolite A T_1 and Calorimetry Analysis. In phase pure zeolite A ($\text{Na}_{12}\text{Al}_{12}\text{Si}_{12}\text{O}_{48} \cdot 27^2\text{H}_2\text{O}$) prior to dehydration, the ratio of water to solid is ca. 0.32 by weight. Of the three rehydrated samples studied here, only the sample with highest loading exceeded this ratio. Neither of the lower loading samples had sufficient $^2\text{H}_2\text{O}$ to fill the pores of zeolite A. The sample

with lowest loading had slightly less than one $^2\text{H}_2\text{O}$ molecule for each two sodalite cages, and the sample with intermediate loading had approximately 4.3 $^2\text{H}_2\text{O}$ molecules per sodalite cage. For both lower loadings, extremely short T_1 values were observed. On the basis of the similarity of the observed T_1 values to those of kanemite, it is reasonable to assume that the water in the lower loading samples is entirely solid state with the ^2H nuclei experiencing rapid tetrahedral jumps. In accordance with this assumption, the T_1 values observed at both magnetic fields for the 0.05 g of $^2\text{H}_2\text{O}/\text{g}$ of zeolite A sample are exactly consistent with $qcc = 193 \text{ kHz}$, $\eta = 0$, and a jumprate $\nu = 5.4 \times 10^8 \text{ s}^{-1}$, but could not be matched within experimental error with the isotropic rotational diffusion model. It should be noted, however, that the uncertainty in the T_1 values ($\pm 0.2 \text{ ms}$) and their limited field dependence (8.3 and 9.2 ms, respectively, at 45.65 and 76.78 MHz) makes the finding for zeolite A somewhat less definitive than that for kanemite.

The existence of solid-state pore water with jumping H nuclei in zeolite A is consistent with observations that H atoms in hydrated H-rho zeolite have high angular mobility but low translational mobility.²⁵ It also is consistent with the observation that water in zeolite A is known to coordinate to Na^+ and to the oxygen atoms in the cage structure in a manner similar to kanemite.

The calorimetric data obtained for $^1\text{H}_2\text{O}$ -hydrated zeolite A are shown in Table 2. The heat evolution observed is again significantly greater than the heat of fusion of water. Although there are other contributions to the observed heat evolution, such as the heat of solvation of the Na^+ ions, enough heat is released to contain contributions from the liquid- to solid-state transformation of water.

Thirsty Glass T_1 and Calorimetry Analysis. ^2H NMR T_1 relaxation times for the central aqueous peak in the spectra of the rehydrated highly porous glass samples are given in Table 2. The T_1 values are consistent with solid water at the surface (with fast tetrahedral jumps of the H nuclei) in fast exchange with liquid water farther from the surface (eq 1).

The calorimetric data obtained for $^1\text{H}_2\text{O}$ -hydrated highly porous glass are shown in Table 2. Little heat was evolved during hydration of the highly porous glass, but this sample also had the longest T_1 values at very low $^2\text{H}_2\text{O}$ loadings. The porous glass also has a very low concentration of counterions in the vicinity of the silicate surface.

Silica Gel T_1 and Calorimetry Analysis. The ^2H NMR T_1 relaxation times for the aqueous peak of the rehydrated silica gel sample are reported in Table 2. As in the case of porous glass and hydrated Ca_3SiO_5 , the T_1 values are consistent with solid water at the surface (with fast tetrahedral jumps of the H nuclei) in fast exchange with liquid water farther from the surface (eq 1).

The heat evolution during hydration of silica gel was less than that for kanemite, zeolite A, and Ca_3SiO_5 , but there are virtually no counterions to solvate and the quantity of heat evolved is still large and consistent with a lesser amount of solid surface water formation.

Limitations and Applications of Equation 1. In principle, if one knows $T_{n,\text{solid}}$ for the solid water next to the surface and the distribution of pore and channel sizes, one can use the experimental $T_{n,\text{observed}}$ and eq 1 to solve for the mole fractions of solid and liquid water. Similarly, one can use eq 1 to determine the $T_{n,\text{solid}}$ for the solid surface water for a given hydrate by extrapolation to zero loading of $^2\text{H}_2\text{O}$, where the mole fraction of the solid water approaches 1. Many studies of this type have been carried out,¹⁻⁴ although none has previously

identified the surface water as a solid in which the H nuclei experience rapid tetrahedral jumps.

It was not possible to estimate mole fractions of solid water for any of the samples except kanemite or rehydrated zeolite A at low $^2\text{H}_2\text{O}$ loadings because the ^2H $T_{1,\text{solid}}$ values of the other samples are not known with certainty. Furthermore, there is considerable variability in the $T_{1,\text{solid}}$ values measured even for kanemite and zeolite A depending on the amount of $^2\text{H}_2\text{O}$ present in the sample (Table 2). This observation is not unexpected. Water molecules exhibit faster C_2 symmetry jumps in some room temperature crystalline hydrates than in others.^{7,8} The variability in the jump rate is sufficient that some room temperature crystalline hydrates are rigid ($\nu \ll qcc$) on the ^2H NMR time scale and some are dynamic ($\nu \gg qcc$).^{7,8} These results suggest that at any temperature the specific jump rate as well as the corresponding T_1 value in the solid state depends on the details of the chemical environment of the water. In the case of kanemite, evaporation of part of the interlayer water resulted in significant, but not order of magnitude, changes in the $T_{1,\text{solid}}$ values. Thus, both the $T_{1,\text{solid}}$ value and the tetrahedral jump rate can vary for the surface water in hydrated porous silicates.

Nevertheless, to give a crude estimate of the "ice-like" solid-state water content of the other samples, the approximation has been used that the T_1 values of the solid water at 45.65 and 76.78 MHz are the same as those determined for kanemite at room temperature. By using this approach it is found that the mole fraction of solid water is ca. 0.27 for the lowest loading of $^2\text{H}_2\text{O}$ in highly porous glass, 0.17 for the lowest loading of $^2\text{H}_2\text{O}$ in silica gel, and 0.27 for the six year old sample of hydrated Ca_3SiO_5 (Table 2).

Other Experiments. Rapid tetrahedral jumps of H nuclei in solid-state water would be expected to produce a translational diffusion coefficient for hydrogen that is larger than that for oxygen. The stray field gradient stimulated echo experiment^{26,27} was used to measure the room temperature translational diffusion coefficient of ^1H and ^{17}O in bulk H_2^{17}O (59.9 atom %, MSD Isotopes lot no. 2249-J) and in fully hardened $^1\text{H}_2^{17}\text{O}$ -hydrated Ca_3SiO_5 two months after mixing. In bulk H_2^{17}O , the translational diffusion coefficients of ^1H and ^{17}O were identical ($2.0 \times 10^{-5} \text{ cm}^2 \text{ s}^{-1}$) within experimental error. The diffusion coefficient of ^1H in the hardened cement mixture two months after mixing was found to be $1.6 \times 10^{-7} \text{ cm}^2 \text{ s}^{-1}$, but the diffusion coefficient for ^{17}O could not be determined because the ^{17}O T_1 and T_2 relaxation times were too short in the hardened cement to measure signal attenuation due to ^{17}O diffusion.

Conclusions

Exhaustive experimental data for five $^2\text{H}_2\text{O}$ -hydrated silicates are presented that are consistent with the hypothesis that room temperature solid-state water forms on and directly adjacent to silicate surfaces. ^2H NMR spectra and T_1 relaxation times show that the ^2H nuclei in the solid-state surface water experience rapid tetrahedral jumps similar to those observed in pure $^2\text{H}_2\text{O}$ ice below the freezing point. Solid-state surface water has been detected during the synthesis of kanemite, during the hydration of Ca_3SiO_5 , and during the rehydration of zeolite A, highly porous glass, and silica gel. The findings are consistent with heat evolution in excess of the heat of fusion of water during the formation of the proposed solid-state water. An alternative hypothesis that the surface water remains in the liquid state does not match the T_1 data. In kanemite and in zeolite A at low $^2\text{H}_2\text{O}$ loadings, the evidence strongly suggests that the water between

silicate surfaces is entirely solid state. In samples such as highly porous glass, silica gel, and hydrated tricalcium silicate, water in the solid state forms only in the vicinity of the silicate surface and is in rapid exchange with liquid state water further from the surface. In hydrated tricalcium silicate, the mole fraction of solid-state water increases dramatically with time as the cement sets and hardens. Distinct ^2H NMR powder spectra observed for silanol $-\text{OH}$ groups in kanemite, rehydrated porous glass, and rehydrated silica gel show that the $-\text{OH}$ groups experience rapid 3-fold jumps or rapid rotational diffusion about the $\text{Si}-\text{O}$ bond, but do not participate in fast exchange with solid- or liquid-state water.

Acknowledgment. We thank Ed Rakiewicz for first suggesting ^2H NMR of $^2\text{H}_2\text{O}$ -hydrated cement, and Stephen Kwan for performing many of the earliest experiments on cement. We thank the Pennsylvania State University for general support.

Supporting Information Available: The Mathematica programs used in the line shape simulations and T_1 calculations (ZIP file). This material is available free of charge via the Internet at <http://pubs.acs.org>.

References and Notes

- (1) D'Orazio, F.; Bhattacharja, S.; Halperin, W. P.; Eguchi, K.; Mizusaki, T. *Phys. Rev. B* **1990**, *42*, 9810.
- (2) Woessner, D. E. *J. Magn. Reson.* **1980**, *39*, 297.
- (3) Letellier, M.; Tinet, D.; Maggion, R.; Fripiat, J. *Magn. Res. Imaging* **1991**, *9*, 709.
- (4) Greener, J.; Peemoeller, H.; Choi, C.; Holly, R.; Reardon, E. J.; Hansson, C. M.; Pintar, M. M. *J. Am. Ceram. Soc.* **2000**, *83*, 623.
- (5) Schmidt-Rohr, K.; Spiess, H. W. *Multidimensional Solid-State NMR and Polymers*; Academic Press: San Diego, CA, 1994.
- (6) Hoatson, G. L.; Vold, R. L. In *Encyclopedia of Nuclear Magnetic Resonance*; Grant, D. M., Harris, R. K., Eds.; Wiley & Sons Scientific: New York, 1996; p 1582.
- (7) Weiss, A.; Weiden, N. In *Advances in Nuclear Quadrupole Resonance*; Smith, J. A. S., Ed.; Heyden & Son Ltd.: London, UK, 1980; Vol. 4.
- (8) Reeves, L. W. In *Progress in N.M.R. Spectroscopy*; Emsley, J. W., Feeney, J., Sutcliffe, L. H., Eds.; Pergamon Press: Oxford, UK, 1969; Vol. 4.
- (9) Lausch, M.; Spiess, H. W. *J. Magn. Reson.* **1983**, *54*, 466.
- (10) Fujara, F.; Wefing, S.; Kuhs, W. F. *J. Chem. Phys.* **1988**, *88*, 6801.
- (11) Torchia, D. A.; Szabo, A. J. *Magn. Reson.* **1982**, *49*, 107.
- (12) Sudmeier, J. L.; Anderson, S. E.; Frye, J. S. *Conc. Magn. Reson.* **1990**, *2*, 197.
- (13) Wittebort, R. J.; Usha, M. G.; Ruben, D. J.; Wemmer, D. E.; Pines, A. *J. Am. Chem. Soc.* **1988**, *110*, 5668.
- (14) Hayashi, S. *J. Mater. Chem.* **1997**, *7*, 1043.
- (15) Garvie, L. A. J.; Devouard, B.; Groy, T. L.; Cámara, F.; Buseck, P. R. *Am. Mineralogist.* **1999**, *84*, 1170.
- (16) Almond, G. G.; Harris, R. K.; Franklin, K. R. *J. Mater. Chem.* **1997**, *7*, 681.
- (17) Rakiewicz, E. F.; Benesi, A. J.; Grutzeck, M. W.; Kwan, S. *J. Am. Chem. Soc.* **1998**, *120*, 6415.
- (18) Taylor, H. F. W. *Cement Chemistry*, 2nd ed.; Thomas Telford: London, UK, 1997.
- (19) Phair, J. W.; Livingston, R. A.; Brown, C. M.; Benesi, A. J. *Chem. Mater.* Accepted for publication.
- (20) Wittebort, R. J.; Olejniczak, E. T.; Griffin, R. G. *J. Chem. Phys.* **1987**, *86*, 5411.
- (21) Mehring, M. In *Encyclopedia of Nuclear Magnetic Resonance*; Grant, D. M., Harris, R. K., Eds.; Wiley & Sons Scientific: New York, 1996; p 2602.
- (22) Bloom, M.; Davis, J. H.; Valik, M. I. *Can. J. Phys.* **1980**, *58*, 1510.
- (23) *Handbook of Chemistry and Physics*, 53rd ed.; Weast, R. C., Ed.; CRC Press: Cleveland, OH, 1972.
- (24) King, T. C.; Dobson, C. M.; Rodger, S. A. *J. Mater. Sci. Lett.* **1988**, *7*, 861.
- (25) Luz, Z.; Vega, A. J. *J. Phys. Chem.* **1987**, *91*, 374.
- (26) Kimmich, R.; Fischer, E. *J. Magn. Reson., Ser. A* **1994**, *106*, 229.
- (27) Geil, B. *Conc. Magn. Reson.* **1998**, *10*, 299.